Peptides 30 (2009) 2365–2373

Contents lists available at ScienceDirect

Peptides

journal homepage: www.elsevier.com/locate/peptides

Epinecidin-1 peptide induces apoptosis which enhances antitumor effects in human leukemia U937 cells

Jyh-Yih Chen [a,b,c,*], Wei-Ju Lin [a], Jen-Leih Wu [d], Guor Mour Her [b], Cho-Fat Hui [d,**]

[a] Marine Research Station, Institute of Cellular and Organismic Biology, Academia Sinica, 23-10 Dahuen Rd., Jiaushi, Ilan 262, Taiwan
[b] Institute of Bioscience and Biotechnology, National Taiwan Ocean University, Keelung 202, Taiwan
[c] Institute of Fisheries Science, National Taiwan University, Taipei 106, Taiwan
[d] Institute of Cellular and Organismic Biology, Academia Sinica, Nankang, Taipei 110, Taiwan

ARTICLE INFO

Article history:
Received 26 July 2009
Received in revised form 23 August 2009
Accepted 23 August 2009
Available online 29 August 2009

Keywords:
Epinecidin-1
Tumor cell inhibition
Lytic peptide

ABSTRACT

Epinecidin-1 is an antimicrobial peptide present in the grouper (*Epinephelus coioides*). In this study, the antitumor activity of a synthetic epinecidin-1 peptide was tested. The *in vitro* results showed that epinecidin-1 inhibited the proliferation of human leukemia U937 cells and increased the ADP/ATP ratio after 24 h of treatment. The DNA fragmentation assay, flow cytometric assay, and caspases-3, -8, and -9 assays indicated that epinecidin-1 could induce apoptosis in U937 cells. Real-time RT-PCR results showed regular increases in tumor necrosis factor (TNF)-α after treatment with 4 μg/ml epinecidin-1 from 4 to 24 h; interleukin (IL)-10, interferon (INF)-r, p53, IL-15, and IL-6 increased after treatment with 2 μg/ml epinecidin-1 for 4–12 h. These results suggest that the epinecidn-1 inhibited U937 cells, induced apoptosis in response to cytokine production, and may have pleiotropic effects on different cells.

1. Introduction

Epinecidin-1, a type of cationic peptide isolated from genes of a complementary (c)DNA library of the grouper (*Epinephelus coioides*), shows antibacterial activities with similar efficiencies for both gram-negative bacteria, gram-positive bacteria, and the fungus, *Trichomonas vaginalis* [24,25]. It consists of 21 amino acid residues, with a structure determined by computer software showing that it contains no disulfide bonds, and which is similar to pleurocidin (amino acids 23–47) in possessing a coiled pattern [8,9]. The cationic synthesized peptide of epinecidin-1 interacts with anionic phospholipids present in bacterial membranes thereby disrupting membrane function [25].

We previously reported that the epinecidin-1 peptide can inhibit the growth of several types of tumor cells through an antitumor effect similar to that of lytic peptides [20]. Moreover, most antimicrobial peptides such as cecropin, melittin, and lactoferricin B cause cytolytic effects on plasma membranes independent of internalization [4,11,13]. From the above description, it was proposed that epinecidin-1 can bind to and disrupt cell membranes resulting in lethal damage. It can interact with membranes of prokaryotic and eukaryotic cells, and it is thought that epinecidin-1 can also interact with the mitochondrial membrane of tumor cells. Previous studies demonstrated that disruption of mitochondria brings about cytochrome *c* and Samc release and activates caspases that can trigger the apoptotic cascade [10,19]. So it seems possible that epinecidin-1 has similar antitumor activities as tachyplesin, GGN6, and PTP7 in inducing apoptosis in tumor cells due to plasma membrane blebbing and DNA fragmentation of peptide-treated tumor cells [6,17].

To explore this possibility, we examined a chemically synthesized peptide of epinecidin-1 in human leukemia U937 cells. These U937 cells are reported to be a model for studying apoptosis in anticancer drug development [7]. We found that this synthetic epinecidin-1 inhibited the proliferation of leukemia U937 cancer cells in a dose-dependent manner by inducing programmed cell death in an *in vitro* test.

2. Materials and methods

2.1. Peptide, cell lines, and MTT viability assay

Epinecidin-1 was synthesized with an amidated C-terminus (GFIFHIIKGLFHAGKMIHGLV-NH_2) by GL Biochem (Shanghai,

* Corresponding author at: Marine Research Station, Institute of Cellular and Organismic Biology, Academia Sinica, 23-10 Dahuen Rd., Jiaushi, Ilan 262, Taiwan. Tel.: +886 920802111; fax: +886 39871035.
** Corresponding author at: Institute of Cellular and Organismic Biology, Academia Sinica, Nankang, Taipei 110, Taiwan. Tel.: +886 227899512; fax: +886 227858059.
E-mail addresses: zoocjy@gate.sinica.edu.tw (J.-Y. Chen), scfhui@gate.sinica.edu.tw (C.-F. Hui).

0196-9781/$ – see front matter © 2009 Elsevier Inc. All rights reserved.
doi:10.1016/j.peptides.2009.08.019

China) at >95% purity following our previous publication [24]. Synthetic peptides were reconstituted in phosphate-buffered saline (PBS; pH 7.4) for the experiments. U937 (human histiocytic lymphoma) cells were obtained from American Type Culture Collection (ATCC; Rockville, MD). Cells were cultured using ATCC-suggested medium and conditions. U937 cells were cultured at 5000 cells/well in 96-well plates and treated with different concentrations of epinecidin-1. The number of viable cells in each well was estimated by adding 10 μl of a 0.5 mg/ml solution of 3-(4,5-dimethylthiazol-2-yl)-2,5-diphenyl tetrazolium bromide (MTT) (Sigma, Louis, MO). Cells were dissolved in 100 μl of solution containing 20% sodium dodecylsulfate (SDS) and 50% dimethyl formamide after cells had been incubated for 240 min at 37 °C. The optical density was measured spectrophotometrically at 570 nm on a microtiter plate reader. Experiments were repeated three times. Results are expressed as a percentage of the inhibition rate of viable cells, and values were subtracted from the PBS-treated group [6].

2.2. Cell variation assay, DNA fragmentation assay, and flow cytometric assay

To detect cell variations, we used acridine orange (AO)/ethidium bromide (EtBr) staining as described before [5]. A DNA fragmentation assay (Suicide Track TM DNA ladder isolation kit) followed the company-provided protocol with no modification (Calbiochem/Novabiochem/Novagen, Darmstadt, Germany; cat. no. AM41). Cytotoxicity was measured by flow cytometry. In brief, U937 cells were plated in 6-well plates at a density of 1×10^6 cells/well and immersed for 24 h. Different concentrations of epinecidin-1 were then added to the cells at a final concentration of 1, 1.5, or 2 μg/ml in a mixture with human tumor necrosis factor (TNF)-α (10 ng/ml) or zVAD (50 μM). There were four groups for the cell

Table 1
Primers used in this paper.

Primer name	Sequence (5′–3′)
Human IL-8-F	CTTTCCACCCCAAATTTATCAAAG
Human IL-8-R	AGAGCTCTCTTCCATCAGAAAGCT
Human IL-12-F	CCTGGACCACCTCAGTTTGG
Human IL-12-R	GACGGCCCTCAGCAGGTT
Human IL-15-F	TCGTATTGTATTGTAGGAGGCATTG
Human IL-15-R	TCAAAGCCACGGTAAATCCTTAA
Human IL-13-F	GCCTCATGGCGCTTTTGTT
Human IL-13-R	AGCTCCCTGAGGGCTGTAGAG
Human IL-6-F	CCTGACCCAACCACAAATGC
Human IL-6-R	CCTTAAAGCTGCGCAGAATGA
Human IL-2-F	CTGCTGGATTTACAGATGATTTTGA
Human IL-2-R	TGGCCTTCTTGGGCATGT
Human IL-10-F	CTGGGTTGCCAAGCCTTGT
Human IL-10-R	AGTTCACATGCGCCTTGATG
Human TGFβ1-F	AACGAAATCTATGACAAGTTCAAGCA
Human TGFβ1-R	AGAGCAACACGGGTTCAGGTA
Human IFN-r-F	TGGCTTAATTCTCTCGGAAACG
Human IFN-r-R	TTTTACATATGGGTCCTGGCAGTA
Human p53-F	GGGTTAGTTTACAATCAGCCACATT
Human p53-R	GGGCCTTGAAGTTAGAGAAAATTCA
Human TNF-α-F	CTCGAACCCCGAGTGACAA
Human TNF-α-R	TTGGCCAGGAGGGCATT
Human GAPDH-F	ACACCCACTCCTCCACCTTT
Human GAPDH-R	TAGCCAAATTCGTTGTCATACC

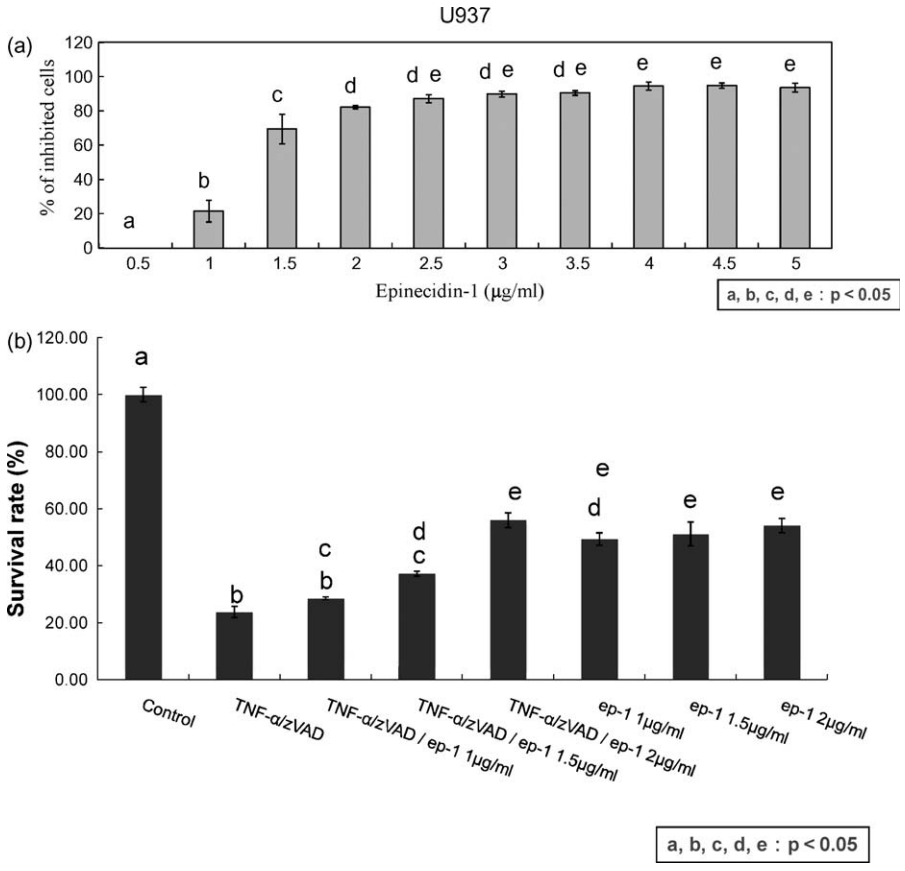

Fig. 1. Effects of epinecidin-1 on U937 cell proliferation. (a) U937 cells were treated with different doses of epinecidin-1 for 24 h, followed by an MTT assay. Each concentration was repeated in eight wells for three independent experiments. (b) U937 cells with different concentrations of epinecidin-1 (1, 1.5, or 2 μg/ml) for 24 h with or without tumor necrosis factor (TNF)-α/zVAD by flow cytometric analysis shows that the survival rate was similar to that of the MTT assay. Data (mean ± SE) with different letters significantly differ ($p < 0.05$) among groups for treatment at different concentrations.

viability assay including one group treated with TNF-α and zVAD; a second group treated with TNF-α, zVAD, and epinecidin-1; a third group treated with epinecidin-1 (1, 1.5, and 2 μg/ml) only; and a fourth group which was not treated with any drugs or peptide. After 24 h, cells were harvested, stained with a propidium iodide (PI) staining kit, and analyzed by flow cytometry (FACSCalibur; Becton Dickinson, San Jose, CA) with laser excitation at 488 nm. Emissions at >590 nm were collected in a linear/log scale fashion. Percentages of cells with fluorescence were determined using standard Modifit and Cell Quest software (Becton Dickinson). To understand the necrotic and apoptotic effects, U937 cells were plated in 24-well plates at a density of 1×10^5 cells/well and immersed for 24 h. U937 cells were divided into groups which were either untreated, treated with epinecidin-1 (0.5, 1, 1.5, 2, 3, and 4 μg/ml), or treated with actinomycin D (0.25 or 0.5 μg/ml) for 2, 4, 8, 12, 19, or 24 h. PI and annexin V (AnxV) were added to the samples and allowed to incubate for 10 min at room temperature. Samples were analyzed by flow cytometry using a Becton Dickinson FACSCalibur using the FL-1 channel to detect the AnxV-FITC and the FL-2 channel for PI.

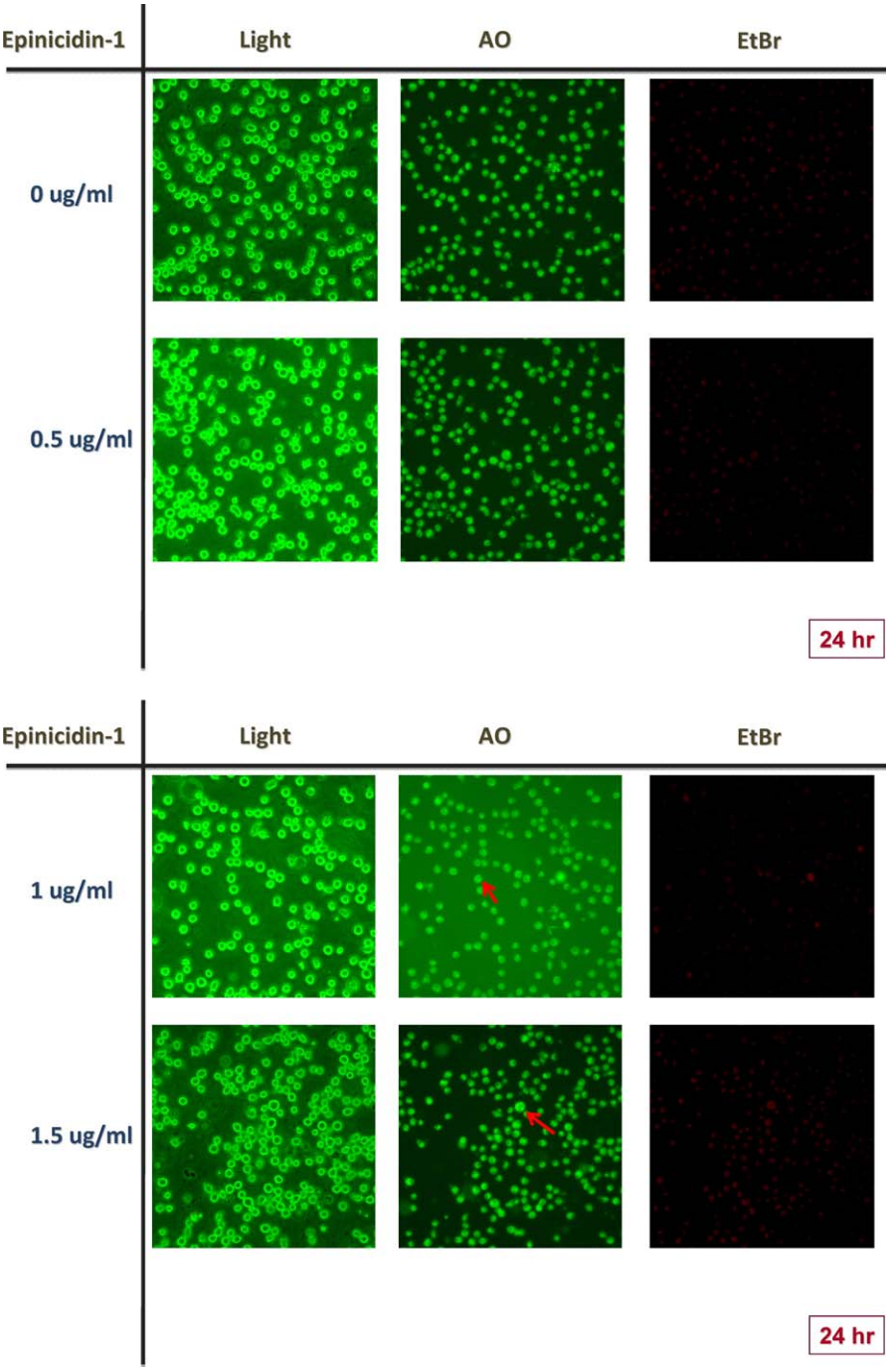

Fig. 2. Morphological variations in U937 cells after treatment with epinecidin-1 for 24 h followed by incubation with or without epinecidin-1. Cells were harvested at the indicated times and then stained with acridine orange (AO)/ethidium bromide (EtBr). AO/EtBr staining produced green nuclei in live cells and orange nuclei in apoptotic cells containing condensed or fragmented chromatin. Arrows indicate apoptotic cells.

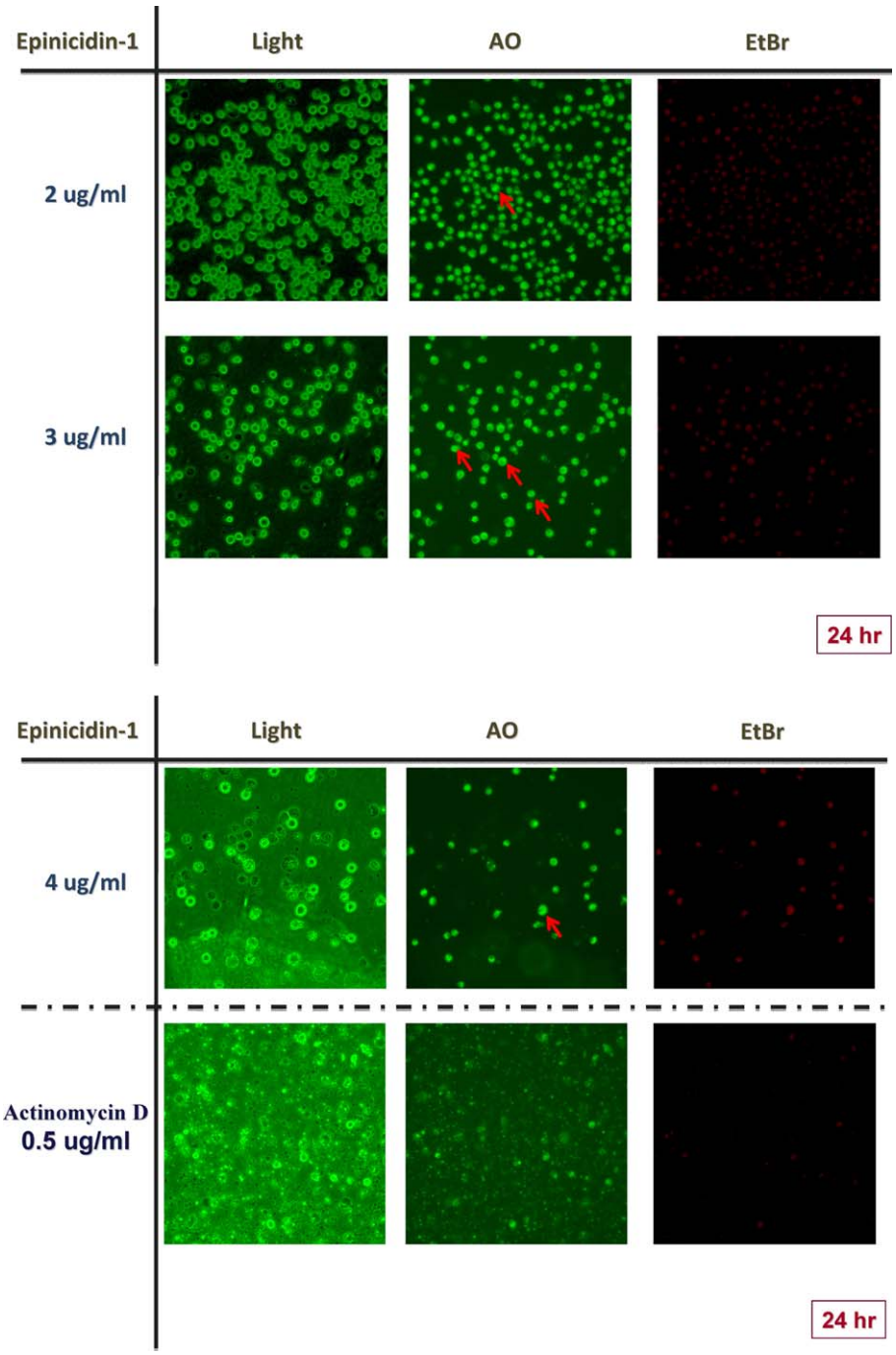

Fig. 2. (*Continued*).

2.3. Caspases-3, -8, and -9 activity assays

Caspases-3, -8, and -9 activities were assayed following the protocol provided by the respective companies. The caspase-3 kit was from BD Pharmingen™, and the Caspase-Glo® 8 Assay and Caspase-Glo® 9 Assay kits were both from Promega (Madison, USA).

2.4. Measurement of the ADP/ATP ratio and real-time reverse-transcription polymerase chain reaction (RT-PCR)

The ADP/ATP ratio in U937 cells was measured by an ADP/ATP ratio assay (BioVision), following a previous publication with no modification [3]. U937 cells were treated with epinecidin-1 (0, 1, 2, and 3 μg/ml), or treated with actinomycin D (0.5 μg/ml) for 4 or 24 h for the mitochondrion activation test. A real-time RT-PCR analysis was used to analyze the gene expressions of TNF-α, INF-r, p53, tumor growth factor (TGF)β1, IL-2, IL-6, IL-8, IL-10, IL-12, IL-13, IL-15, and glyceraldehyde 3 phosphate dehydrogenase (GAPDH). The primers used are shown in Table 1, and GAPDH was used as the reference gene. U937 cells were treated with epinecidin-1 (0, 2, or 4 μg/ml) for 4, 8, 12, or 24 h for the real-time PCR test, and the real-time PCR experimental conditions were the same as those described by Lin et al. [20]. The real-time RT-PCR was performed in triplicate for each experimental group.

3. Results

3.1. In vitro cytotoxicity and epinecidin-1-evoked apoptosis function in U937 cells

As shown in Fig. 1a, epinecidin-1 demonstrated a significant dose-dependent cytotoxic effect against U937 cells. Epinecidin-1 at 2–5 μg/ml proved to be the most effective at inhibiting U937 cells according to the MTT assay. Our flow cytometric results revealed that incubation of U937 cells with different concentrations (1, 1.5, or 2 μg/ml) of epinecidin-1 for 24 h with or without TNF-α/zVAD produced survival rates similar to those of the MTT assay (Fig. 1b). These results provide strong evidence that epinecidin-1 was responsible for the death of the cells, and led us to perform further experiments to understand the dose-dependency of epinecidin-1-induced U937 apoptosis. In order to quantify the degree of apoptosis in U937 cells, we used an EtBr/AO morphological staining method to differentiate live and apoptotic cells by nuclear staining color. In our results, an increase in the concentration of epinecidin-1 produced an increase in orange color (Fig. 2). As is generally known, the method of EtBr/AO staining shows nuclei of live cells as green, while nuclei of apoptotic cells containing condensed or fragmented chromatin appear orange. With 0 μg/ml treatment, we found no apoptotic cells after 24 h of treatment. In contrast, cells treated with 4 μg/ml epinecidin-1 showed an apoptotic pattern. These results suggest that the degree of apoptosis observed in these studied cells was related to epinecidin-1 inhibition of U937 cells.

3.2. The ADP/ATP ratio increases after 24 h of treatment with 3 μg/ml epinecidin-1

Inasmuch as epinecidin-1 exhibits significant inhibitory activity in U937 cells, these results suggest that the degree of apoptosis observed in these studies was related to mitochondrial function. To test this hypothesis, we next incubated U937 cells with epinecidin-1 for 4 or 24 h. Because ATP synthesis depends on the mitochondrial membrane potential, mitochondrial dysfunction produced by epinecidin-1 should cause a rapid increase in the ADP/ATP ratio (Fig. 3). Accordingly, the ADP/ATP ratio significantly increased within 24 h after 3 μg/ml treatment. In contrast, after treatment with 0.5 μg/ml actinomycin D for 24 h, there was a significant increase in the ADP/ATP ratio compared to 4 h of treatment.

3.3. Epinecidin-1 induces apoptosis in U937 cells

The mitochondrial dysfunction after epinecidin-1 treatment suggests that mitochondria have a role in initiating apoptosis from our results. We then examined DNA fragmentation in epinecidin-1-treated cells following incubation for 24 h with different concentrations of epinecidin-1. DNA fragmentation was readily apparent at 1.5–3 μg/ml and clearly visible by agarose gel electrophoresis (Fig. 4a). In order to understand whether the reduction in cell viability was due to apoptosis, we confirmed that cell death occurred via apoptosis by the FACS analysis after AnxV-FITC/PI staining (Fig. 4b and c). Flow cytometry is an excellent method to differentiate live, early-apoptotic, and late-apoptotic cells. Therefore, co-treatment of U937 cells with PI and AnxV allows the discrimination of early apoptotic (AnxV-positive/PI-negative) from terminal stages of apoptosis (AnxV-positive/PI-positive). As shown in Fig. 4b, apoptotic cell populations increased following treatment of cells with epinecidin-1 (4 μg/ml) at 2–24 h. In contrast, necrotic cells treated with epinecidin-1 (3 or 4 μg/ml) were observed to have decreased at 2–24 h (Fig. 4c).

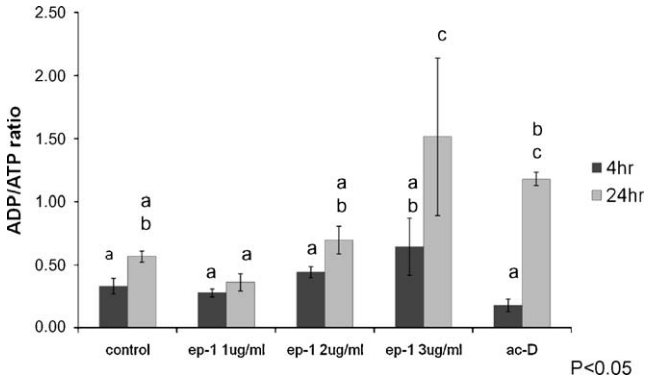

Fig. 3. Mitochondrion activation analysis in U937 cells. Concentration effects of U937 cells incubated with different dosages of epinecidin-1 for 4 or 24 h. The ADP/ATP ratio suggested that the cellular preparation exhibited a significant level of apoptosis. Each bar represents the mean value from three determinations with the standard error (SE). Data (mean ± SE) with different letters significantly differ ($p < 0.05$) among treatments.

Thus, these results clearly show that treating U937 cells with epinecidin-1 caused virtually all cells to undergo some degree of apoptosis.

3.4. Epinecidin-1 activates caspases-3, -8, and -9 within 4 h and inactivates them after 24 h

Mitochondrial damage is well known to cause activation of caspase-9 and then downstream to induce apoptosis by caspase-3. We therefore evaluated epinecidin-1s involvement in caspase activation. As expected, epinecidin-1 (3 μg/ml) activated caspases-3, -8, and -9 in U937 cells, with each compound's activity reaching 3–3.5-fold at 4 h of treatment (Fig. 5a–c). Contrary to expectations, epinecidin-1 significantly inactivated caspases-3, -8, and -9 after 24 h of treatment. Collectively, these results led to the conclusion that epinecidin-1 activates caspases-3, -8, and -9 in U937 cells with 4 h of treatment.

3.5. Gene expressions increase in U937 cells after treatment with the epinecidin-1 peptide

To investigate the effects of epinecidin-1 on U937 cell function, we performed a real-time RT-PCR analysis of TNF-α, INF-r, p53, TGFβ1, IL-2, IL-6, IL-8, IL-10, IL-12, IL-13, and IL-15. As shown in Fig. 6, we observed regular increases in TNF-α of cells treated with 4 μg/ml epinecidin-1 from 4 to 24 h; IL-10, INF-r, p53, IL-15, and IL-6 showed regular increases after treatment with 2 μg/ml epinecidin-1 from 4 to 12 h. These results suggest that epinecidin-1-treated U937 cells induced cytokine production and may have pleiotropic effects on different cells.

4. Discussion

It was demonstrated that the antitumor activity of epinecidin-1 is similar to that of lytic peptides [20]. The mechanism of the apoptotic function underlying the corresponding *in vitro* activity of epinecidin-1 has not been reported. Nonetheless, it was suggested that epinecidin-1 exerts its antitumor activities by different mechanisms in different cell types. In the present study, we found that epinecidin-1 was cytotoxic against the U937 cell line *in vitro* according to our MTT and flow cytometric analyses. Our earlier studies revealed that epinecidin-1 inhibited cell growth in a highly aggressive fibrosarcoma cell line, HT-1080, although we failed to

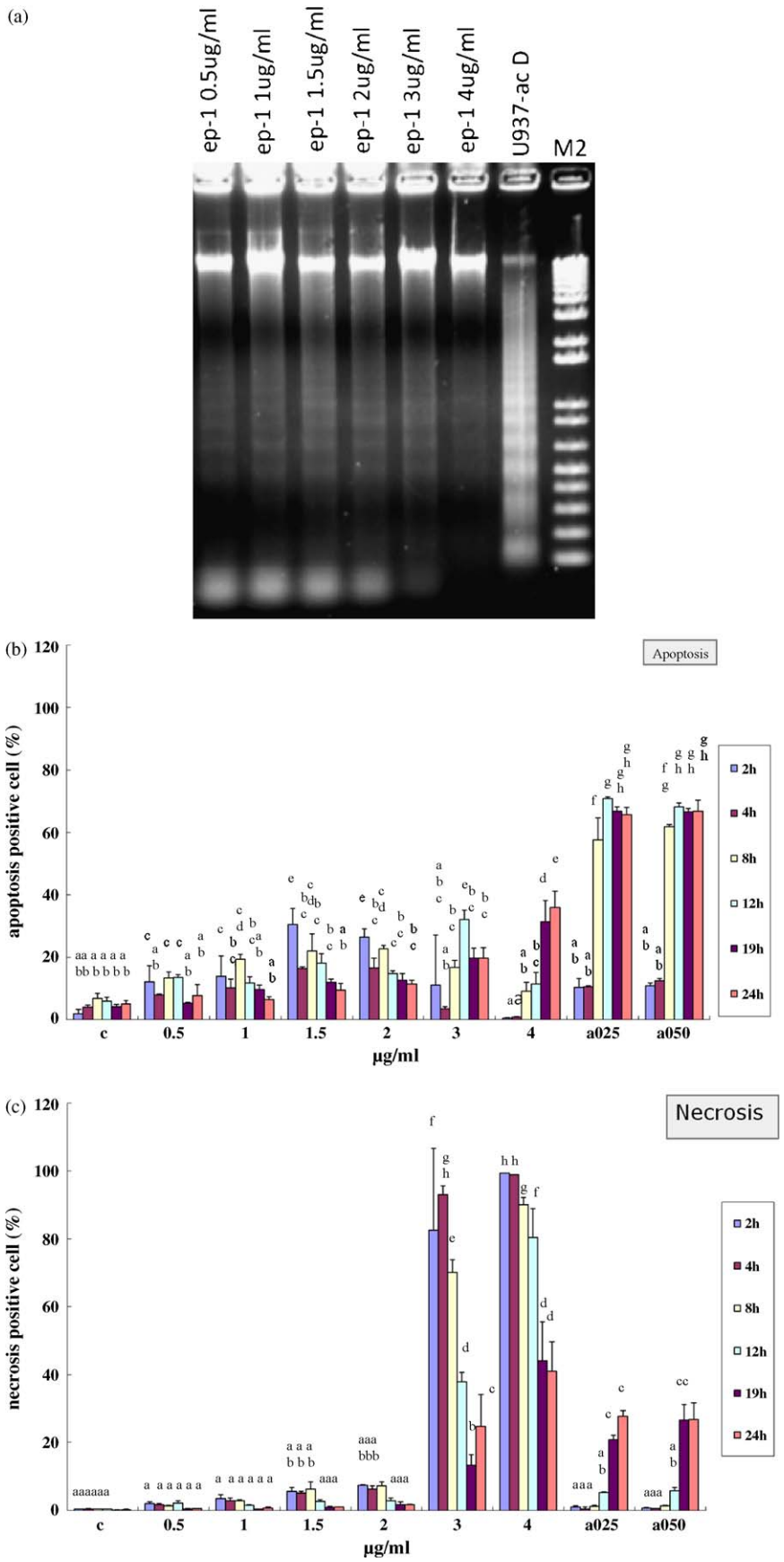

Fig. 4. Epinecidin-1 induces apoptotic cell death in human leukemia U937 cells. (a) After treatment with different concentrations of epinecidin-1 for 24 h, DNA ladder formation was observed in U937 cells. Actinomycin D (0.5 μg/ml) was used as the control group. (b) Induction of apoptosis in U937 cells by epinecidin-1. U937 cells were treated with different concentrations of epinecidin-1 for different times, and U937 cells were collected to conduct the annexin V-propidium iodide assay, as described in

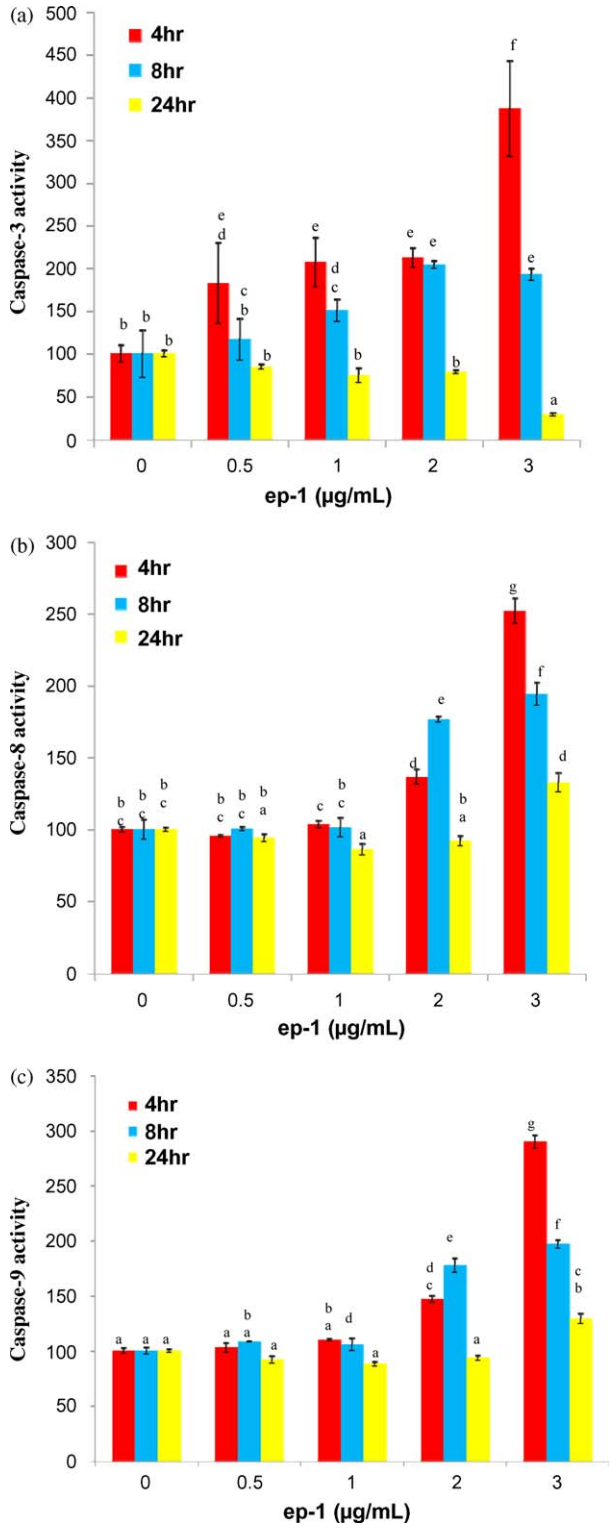

Fig. 5. Effects of epinecidin-1 on caspase activation. Caspases involved in epinecidin-1-induced apoptosis were identified as caspases-3 (a), -8 (b), and -9 (c). The functional relevance of caspases-3, -8, and -9 activation during epinecidin-1-induced apoptosis was evaluated by a caspase assay kit. Each bar represents the mean value from three determinations with the standard error (SE). Data (mean ± SE) with different letters significantly differ ($p < 0.05$) among treatments.

reduce HT1080 cell growth or metastasis in athymic mice. Moreover, antimicrobial peptides are amphipathic peptides with cytotoxic specificity for negatively charged prokaryotic membranes and which also disrupt mitochondria to selectively induce apoptosis in tumor cells [1,22,26]. Epinecidin-1 was able to selectively induce apoptosis in U937 cancer cells and induce apoptosis in a caspase-dependent manner as revealed by the use of zVAD that strongly prevents any pro-apoptogenic activity according to the flow cytometric analysis and EtBr/AO staining. In contrast, expression of other antimicrobial peptides such as prepromelittin in cancer cells resulted in a slight reduction in the frequency of tumor formation [28], suggesting that not all antimicrobial peptides possess the ability to inhibit tumor formation.

The present observations in the U937 cell line reveal a correlation between epinecidin-1 treatment and mitochondrial activity as reflected by ATP levels and the energy status. Mitochondria are reported to play a key role in regulating apoptosis [14]. Mitochondrial dysfunction includes loss of the mitochondrial membrane potential, permeability transition, and induction of apoptosis associated with movement of cytochrome c from mitochondria to the cytosol [15,27]. These data suggest that apoptosis induced by epinecidin-1 is dependent on the mitochondrial membrane integrity, which has been reported to be disrupted due to opening of the permeability transition pores. Disruption of the mitochondrial membrane potential is thought to be a common event in the induction of apoptosis [18]. In another report, agents which caused depletion of ATP induced apoptosis and enhanced the effect of chemotherapy in tumor-bearing mice [23]. Our data show a significant correlation between the ADP/ATP ratio and the degree of DNA fragmentation as measured by gel electrophoresis. As fragmentation of DNA is a late event in apoptosis and measurement of the ADP:ATP ratio in cell lines can be used as an indicator of cell viability, necrosis, and apoptosis [2], one could conclude that variations in the ADP/ATP ratio are involved in late apoptosis in epinecidin-1-treated U937 cells.

Our results suggest that epinecidin-1 upregulates apoptosis related to caspases-3, -8, and -9 activation at 4 and 8 h. Presumably, this resulted from the release of cytochrome *c*, which activated downstream caspase-9 and then caspases-3, -7, and -6 [16,21]. In addition, we found that one of the members of the death receptor pathway (caspase-8) was also upregulated after epinecidin-1 (2 or 3 μg/ml) treatment for 4 and 8 h. Epinecidin-1 might bind to some death receptor(s) and trigger the death receptor signal transduction pathway. Thus, epinecidin-1 may have multiple effects on U937 cells in terms of the mitochondrial pathway and the death receptor pathway. There are several reports regarding the two signal transduction pathways of gossypol and RGD-tachyplesin [6,29].

Our results suggest that epinecidin-1 upregulates interleukin-related genes. Therefore, epinecidin-1s involvement in interleukin's function was indicated by the real-time RT-PCR analysis in the presence of epinecidin-1 treatment. The important interleukin which highly increased after epinecidin-1 treatment was IL-10. IL-10 inhibits cytokine synthesis by a Th2 clone and inhibits IFN-γ expression in Th1 cells [12]. In the present study, we found that epinecidin-1 not only possessed an apoptosis function in U937 cells but also stimulated interleukin expression, suggesting that epinecidin-1 may have the potential to serve as a drug for therapy against human leukemia U937 cells.

Section 2. (c) The necrosis-positive cell treatment was the same as that described in (b). Each bar represents the mean value from three determinations with the standard error (SE). Data (mean ± SE) with different letters significantly differ ($p < 0.05$) among treatments.

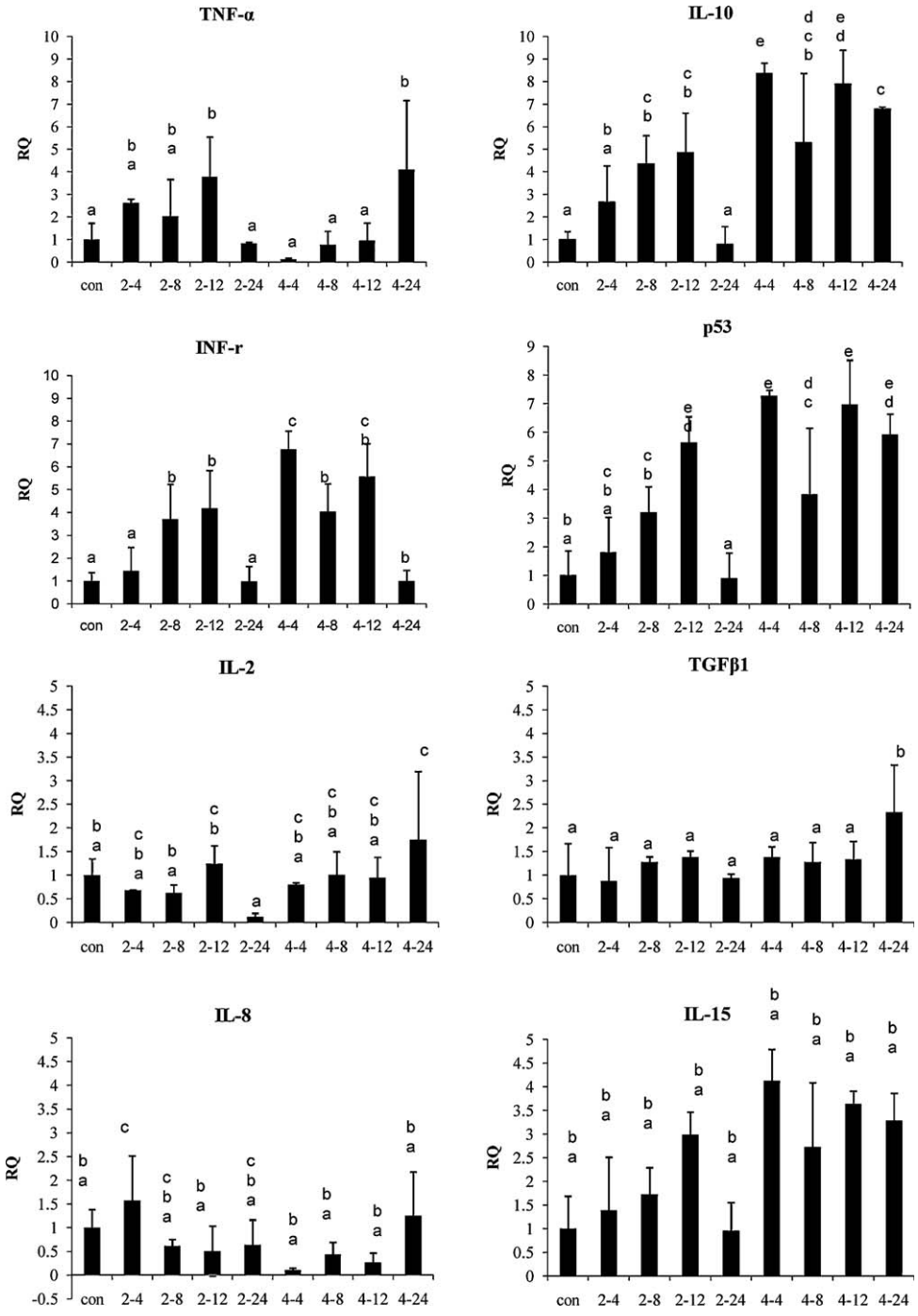

Fig. 6. Quantification of transcript levels by comparative real-time RT-PCR. RNA from U937 cells was co-treated with 2 or 4 μg/ml epinecidin-1. The control group (con) was not treated with peptide. Samples were collected after treatment for 4, 8, 12, and 24 h. Transcript abundance, normalized to GAPDH expression, is expressed as the relative expression and graphed on a rational scale. Each bar represents the mean value from three determinations with the standard error. Data (mean ± SE) with different letters significantly differ ($p < 0.05$) among treatments. An example of an *x*-coordinate is 2-24, where 24 is the number of hours, and 2 is the dosage (μg/ml) for epinecidin-1; i.e., 2-24 was treated with 2 μg/ml epinecidin-1 for 24 h.

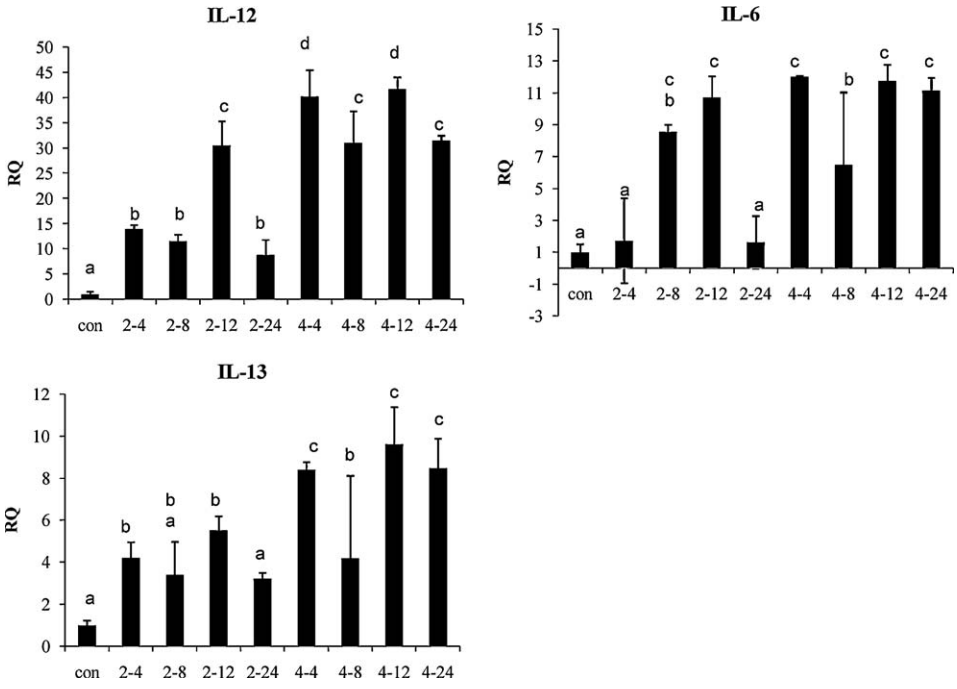

Fig. 6. (*Continued*).

Acknowledgements

This work was supported by a grant from the Marine Research Station, Institute of Cellular and Organismic Biology, Academia Sinica.

References

[1] Béven L, Castano S, Dufourcq J, Wieslander A, Wróblewski H. The antibiotic activity of cationic linear amphipathic peptides: lessons from the action of leucine/lysine copolymers on bacteria of the class Mollicutes. Eur J Biochem 2003;270:2207–17.
[2] Bradbury DA, Simmons TD, Slater KJ, Crouch SP. Measurement of the ADP:ATP ratio in human leukaemic cell lines can be used as an indicator of cell viability, necrosis and apoptosis. J Immunol Methods 2000;240:79–92.
[3] Chan JY, Chan SH, Dai KY, Cheng HL, Chou JL, Chang AY. Cholinergic-receptor-independent dysfunction of mitochondrial respiratory chain enzymes, reduced mitochondrial transmembrane potential and ATP depletion underlie necrotic cell death induced by the organophosphate poison mevinphos. Neuropharmacology 2006;51:1109–19.
[4] Chan SC, Hui L, Chen HM. Enhancement of the cytolytic effect of anti-bacterial cecropin by the microvilli of cancer cells. Anticancer Res 1998;18:4467–74.
[5] Chen JY, Lin WJ, Lin TL. A fish antimicrobial peptide, tilapia hepcidin TH2-3, shows potent antitumor activity against human fibrosarcoma cells. Peptides 2009;30(9):1636–42.
[6] Chen Y, Xu X, Hong S, Chen J, Liu N, Underhill CB, et al. RGD-Tachyplesin inhibits tumor growth. Cancer Res 2001;61:2434–8.
[7] Choi YH. Apoptosis of U937 human leukemic cells by sodium butyrate is associated with inhibition of telomerase activity. Int J Oncol 2006;29:1207–13.
[8] Cole AM, Weis P, Diamond G. Isolation and characterization of pleurocidin, an antimicrobial peptide in the skin secretions of winter flounder. J Biol Chem 1997;272:12008–13.
[9] Cole AM, Darouiche RO, Legarda D, Connell N, Diamond G. Characterization of a fish antimicrobial peptide: gene expression, subcellular localization, and spectrum of activity. Antimicrob Agents Chemother 2000;44:2039–45.
[10] Du C, Fang M, Li Y, Li L, Wang X. Smac, a mitochondrial protein that promotes cytochrome c-dependent caspase activation by eliminating IAP inhibition. Cell 2000;102:33–42.
[11] Eliassen LT, Berge G, Leknessund A, Wikman M, Lindin I, Løkke C, et al. The antimicrobial peptide, lactoferricin B, is cytotoxic to neuroblastoma cells in vitro and inhibits xenograft growth in vivo. Int J Cancer 2006;119:493–500.
[12] Fiorentino DF, Bond MW, Mosmann TR. Two types of mouse T helper cell. IV. Th2 clones secrete a factor that inhibits cytokine production by Th1 clones. J Exp Med 1989;170:2081–95.
[13] Gonçalves E, Kitas E, Seelig J. Structural and thermodynamic aspects of the interaction between heparan sulfate and analogues of melittin. Biochemistry 2006;45:3086–94.
[14] Gottlieb RA. Role of mitochondria in apoptosis. Crit Rev Eukaryot Gene Expr 2000;10:231–9.
[15] Huang F, Nie C, Yang Y, Yue W, Ren Y, Shang Y, et al. Selenite induces redox-dependent Bax activation and apoptosis in colorectal cancer cells. Free Radic Biol Med 2009;46:1186–96.
[16] Kaufmann SH, Earnshaw WC. Induction of apoptosis by cancer chemotherapy. Exp Cell Res 2000;256:42–9.
[17] Kim S, Kim SS, Bang YJ, Kim SJ, Lee BJ. In vitro activities of native and designed peptide antibiotics against drug sensitive and resistant tumor cell lines. Peptides 2003;24:945–53.
[18] Kroemer G, Zamzami N, Susin SA. Mitochondrial control of apoptosis. Immunol Today 1997;18:44–51.
[19] Li H, Kolluri SK, Gu J, Dawson MI, Cao X, Hobbs PD, et al. Cytochrome c release and apoptosis induced by mitochondrial targeting of nuclear orphan receptor TR3. Science 2000;289:1159–64.
[20] Lin WJ, Chien YL, Pan CY, Lin TL, Chen JY, Chiu SJ, et al. an antimicrobial peptide from fish (Epinephelus coioides) which has an antitumor effect like lytic peptides in human fibrosarcoma cells. Peptides 2009;30:283–90.
[21] Liu G, Shao W, Huang X, Wu H, Tang W. Structural studies of imidazole-cytochrome c: resonance assignments and structural comparison with cytochrome c. Biochim Biophys Acta 1996;1277:61–82.
[22] Mai JC, Mi Z, Kim SH, Ng B, Robbins PD. A proapoptotic peptide for the treatment of solid tumors. Cancer Res 2001;61:7709–12.
[23] Martin DS, Schwartz GK. Chemotherapeutically induced DNA damage, ATP depletion, and the apoptotic biochemical cascade. Oncol Res 1997;9:1–5.
[24] Pan CY, Chen JY, Cheng YS, Chen CY, Ni IH, Sheen JF, et al. Gene expression and localization of the epinecidin-1 antimicrobial peptide in the grouper (Epinephelus coioides), and its role in protecting fish against pathogenic infection. DNA Cell Biol 2007;26:403–13.
[25] Pan CY, Chen JY, Lin TL, Lin CH. In vitro activities of three synthetic peptides derived from epinecidin-1 and an anti-lipopolysaccharide factor against Propionibacterium acnes, Candida albicans, and Trichomonas vaginalis. Peptides 2009;30:1058–68.
[26] Papo N, Shai Y. Can we predict biological activity of antimicrobial peptides from their interactions with model phospholipid membranes? Peptides 2003;24:1693–703.
[27] Tang L, Zhang Y, Jobson HE, Li J, Stephenson KK, Wade KL, et al. Potent activation of mitochondria-mediated apoptosis and arrest in S and M phases of cancer cells by a broccoli sprout extract. Mol Cancer Ther 2006;5:935–44.
[28] Winder D, Günzburg WH, Erfle V, Salmons B. Expression of antimicrobial peptides has an antitumour effect in human cells. Biochem Biophys Res Commun 1998;242:608–12.
[29] Zhang M, Liu H, Guo R, Ling Y, Wu X, Li B, et al. Molecular mechanism of gossypol-induced cell growth inhibition and cell death of HT-29 human colon carcinoma cells. Biochem Pharmacol 2003;66:93–103.